Artificial intelligence-based prediction of neurocardiovascular risk score from retinal swept-source optical coherence tomography–angiography

C. Germanese, A. Anwer, P. Eid, L.-A. Steinberg, C. Guenancia, Pierre Henry Gabrielle, Catherine Creuzot-Garcher, F. Meriaudeau, Louis Arnould

scientific reports

Check for updates

OPEN

Artificial intelligence-based prediction of neurocardiovascular risk score from retinal swept-source optical coherence tomography–angiography

C. Germanese[1,2], A. Anwer[2], P. Eid[1], L.-A. Steinberg[1], C. Guenancia[3,4], P.-H. Gabrielle[1,5], C. Creuzot-Garcher[1,5], F. Meriaudeau[2] & L. Arnould[1,4]✉

The recent rise of artificial intelligence represents a revolutionary way of improving current medical practices, including cardiovascular (CV) assessment scores. Retinal vascular alterations may reflect systemic processes such as the presence of CV risk factors. The value of swept-source retinal optical coherence tomography–angiography (SS OCT-A) imaging is significantly enhanced by image analysis tools that provide rapid and accurate quantification of vascular features. We report on the interest of using machine-learning (ML) and deep-learning (DL) models for CV assessment from SS OCT-A microvasculature imaging. We assessed the accuracy of ML and DL algorithms in predicting the CHA_2DS_2-VASc neurocardiovascular score based on SS OCT-A retinal images of patients from the open-source RASTA dataset. The ML and DL models were trained on data from 491 patients. The ML models tested here achieved good performance with area under the curve (AUC) values ranging from 0.71 to 0.96. According to a classification into two neurocardiovascular risk groups, the EfficientNetV2-B3, a well suited DL model for retinal OCT-A images, predicted risk correctly in 68% of cases, with a mean absolute error (MAE) of approximately 0.697. Our models enable a confident prediction of the CHA_2DS_2-VASc score from SS OCT-A imaging, which could be a useful tool contributing to the assessment of neurocardiovascular profiles in the future.

Keywords OCT-A, CHA_2DS_2-VASc, Machine learning, Deep learning, Neurocardiovascular, Prediction

With approximately 17.9 million deaths every year[1], cardiovascular diseases (CVD) are the leading cause of death worldwide, and the assessment of cardiovascular (CV) risk plays a major role in their prevention. Today, CV risk profiles can be estimated with numerous validated score models such as the Framingham Risk Score (FRS), the American Heart Association risk score (AHA risk score), or the SCORE2[2–4]. Nevertheless, these clinical scores do not take into account personalized vascular conditions, and recurrent neurovascular and cardiovascular events are still difficult to predict[5,6]. We previously demonstrated through a conventional regression approach in post-myocardial infarction patients in the EYE-MI study that retinal optical coherence tomography–angiography (OCT-A) could be an effective tool for predicting cardiovascular risk scores[7]. Swept-source OCT–angiography (SS OCT-A) technology, with more thorough retinal microvasculature description and better resolution, could be used to refine the EYE-MI pilot study results in patients with broader phenotypes[8–13]. Moreover, the CHA_2DS_2-VASc score, a cardioembolic risk score[14], may better reflect the connection between the retinal, neurovascular, and cardiovascular systems. The role of advanced imaging analysis is becoming increasingly important in daily clinical practice and biomedical research due to the recent advancements in oculomics[15] and other artificial intelligence (AI)-based image analysis methods[16]. In the framework of open-source datasets in ophthalmology[17], we previously published the Retinal oct-Angiography and cardiovascular

[1]Department of Ophthalmology, Dijon University Hospital, Dijon, France. [2]Institut de Chimie Moléculaire Université de Bourgogne (ICMUB), Imagerie Fonctionnelle et moléculaire et Traitement des Images Médicales (IFTIM), Burgundy University, EA 7535, Dijon, France. [3]Department of Cardiology, Dijon University Hospital, Dijon, France. [4]Pathophysiology and Epidemiology of Cerebro-Cardiovascular Diseases (PEC2), Université de Bourgogne, EA 7460, Dijon, France. [5]Eye and Nutrition Research Group, CSGA, UMR 1324 INRA, 6265 CNRS, Burgundy University, Dijon, France. ✉email: louis.arnould@chu-dijon.fr

Risk Factor	Score
Congestive heart failure / Left ventricular dysfunction	1
Hypertension	1
Age ≥ 75 years	2
Diabetes mellitus	1
Stroke/TIA/TE	2
Vascular disease (prior myocardial infarction, peripheral artery disease, or aortic plaque)	1
Age 65–74 years	1
Sex category (i.e., female gender)	1

Table 1. CHA_2DS_2-VASc point-based scoring system.

Subject area	Biomedical imaging, ophthalmology
More specific subject area	Retinal OCT-A volume analysis for cardiovascular risk prediction
Type of data	Image, CSV
How data were acquired	Swept-source OCT-A Instrument name: PLEX Elite 9000® (Carl Zeiss Meditec Inc., Dublin, OH, USA)
Data format	DICOM for volumes, Bitmap for en face images
Experimental factors	Pupillary dilatation with tropicamide 0.5% if signal strength < 8/10
Experimental features	Macular angiography 6 × 6-mm
Main data source location	University Hospital of Dijon, Dijon 21000, France
Data accessibility	https://rasta.u-bourgogne.fr/

Table 2. Specifications table.

STAtus (RASTA) dataset[18]. It combined SS OCT-A retinal imaging and CHA_2DS_2-VASc score calculation in patients with various conditions (e.g., diabetes mellitus, giant cell arthritis, dyslipidemia, and ischemic CVD) and accurate phenotype. Recent studies using deep-learning (DL) convolutional neural networks (CNNs) have associated retinal photographs with several CVD risk factors, including diabetes mellitus, blood pressure, body mass index (BMI), smoking, and glycated-hemoglobin level[19–22]. Nevertheless, the literature is sparse regarding the interest of SS OCT-A for artificial intelligence-based prediction of the neurocardiovascular risk score.

The purpose of this study was to train and validate machine-learning- (ML) and DL-based models capable of predicting neurocardiovascular risk scores (CHA_2DS_2-VASc score) using the detection method from SS OCT-A acquisitions in the RASTA dataset.

Methods

Neurocardiovascular risk profile

We used the CHA_2DS_2-VAS_C score (Table 1) as the score for neurocardiovascular risk assessment. It is an embolic risk stratification tool originally used to assess the risk of stroke in patients with non-valvular atrial fibrillation[14]. It has been recently presented as an effective model for patients without atrial fibrillation[23–29]. In contrast to other CV risk scores, it does not need any biological sampling.

Dataset

We previously published the Retinal oct-Angiography and cardiovascular STAtus (RASTA) dataset[18], which was acquired from February 2018 to June 2023 in the Department of Ophthalmology at the University Hospital of Dijon, France. The RASTA dataset was anonymized and processed in accordance with the rules established by the Ethics Committee of the University Hospital of Dijon. The RASTA dataset is hosted and publicly available at https://rasta.u-bourgogne.fr/.

We assembled a cross-sectional set of retinal SS OCT-A images consisting of en face images and angiocubes combined with clinical and demographic characteristics from healthy and at-risk patients with complete clinical CV phenotypes.

Information on data accessibility and specifications is provided in Table 2. Each participant was included in one of two groups according to their neurocardiovascular risk category following the risk scheme used for RASTA (Table 3):

Low neurocardiovascular risk – CHA_2DS_2-VASc = [0; 1]

Intermediate–high neurocardiovascular risk – CHA_2DS_2-VASc = [2; 9].

For each participant, corresponding images of the SS OCT-A 6 × 6-mm acquisitions were obtained with the PLEX Elite 9000® device (Carl Zeiss Meditec Inc., Dublin, OH, USA). En face images (Fig. 1) were based on the plexuses. Moreover, quantitative variables from the 2D SS OCT-A images were available and represented the different measurable characteristics of each patient's superficial and deep retinal vascular plexuses. These

Risk scheme	Low risk [0 ;1]	Intermediate-high risk [2 ;9]
RASTA (2023)	One or no combination risk factor	At least 1 definitive risk factor and 1 or no combination risk factor, or ≥ 2 combination risk factors

Table 3. Risk scheme used for neurocardiovascular risk stratification. Definitive risk factors: previous stroke/TIA/TE, age > 75. Combination risk factors: heart failure/left ventricular ejection fraction ≤ 40%, hypertension, diabetes, vascular disease, female sex, age 65–74.

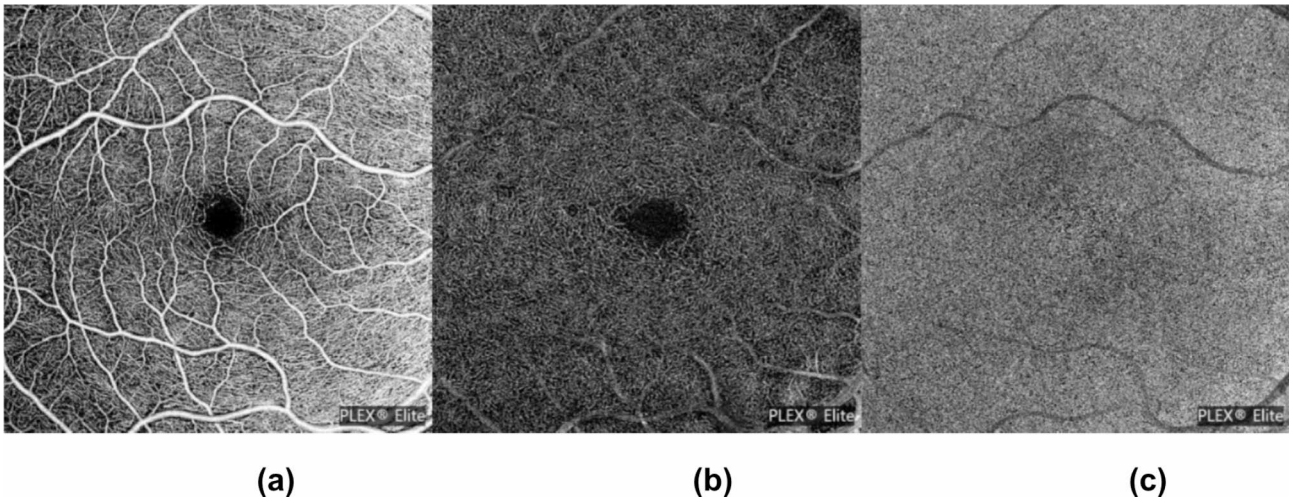

Fig. 1. Right eye en face images of (**a**) superficial plexus, (**b**) deep plexus, and (**c**) choriocapillaris plexus.

quantitative variables were calculated using the ARI Network segmentation and analysis platform developed by the manufacturer Carl Zeiss Meditec Inc.

Machine-learning design

To develop the models, we worked with raw data of 11 CV risk factors including age, gender, diabetes, smoking, and 15 quantitative variables obtained from en face SS OCT-A images (Fig. 2; Table 4). These quantitative variables represent the different measurable characteristics of each patient's superficial and deep retinal vascular plexuses. We used all the quantitative variables of each eye as an independent feature, and thus we finally had 30 retinal quantitative data for each row when information for both eyes was available. These quantitative variables were calculated using the ARI Network segmentation and analysis platform developed by the manufacturer Carl Zeiss Meditec Inc. as described above. The neurocardiovascular risk category was the target.

We built and evaluated four ML algorithms and compared their results: decision tree, random forest (RF), support vector machines (SVM), and logistic regression. Then, given the multivariate and multidimensional nature of the data, we conducted a principal component analysis using Pearson's correlation coefficient to eliminate the effect of scale in the data, moving from a space of 41–19 dimensions for a cumulative variability over 95% (Fig. 3).

Machine-learning model assessment

Due to the limited and imbalanced number of images in the RASTA dataset, a normal train–test split was not possible. Therefore, we employed the k-fold cross-validation method. We opted for a two-stage cross-validation procedure with k = 5 and then with k = 10 (Fig. 4).

Deep-learning network design

We employed cutting-edge DL methodologies to automate the assessment of neurocardiovascular risk using microvascular imaging. Our approach involved constructing a deep convolutional network with the EfficientNetV2 architecture[30] as the backbone, a convolutional neural network (CNN) architecture specifically designed for classification tasks. EfficientNetV2 employs a compound scaling strategy that simultaneously increased the model's depth, width, and resolution. In our implementation, we used the EfficientNetV2-B3 backbone pre-trained on the ImageNet dataset. Input images were resized to a resolution of $300 \times 300 \times 3$ pixels. The network architecture incorporated three dense layers, with a 20% dropout between each layer. The top two dense layers employed rectified linear unit (ReLU) activation, while the final layer utilized SoftMax activation, producing two outputs corresponding to the probabilities of different neurocardiovascular risk category. The network architecture is illustrated in Fig. 5. Following the initial training phase, we performed fine-tuning by unfreezing the last 20 layers and retraining the model. Fine-tuning involved making subtle adjustments to the pre-trained model's weights or parameters using data from the target task. Due to the limited number of images in one of the two categories in the RASTA dataset, we employed the stratified k-fold cross-validation with k = 5

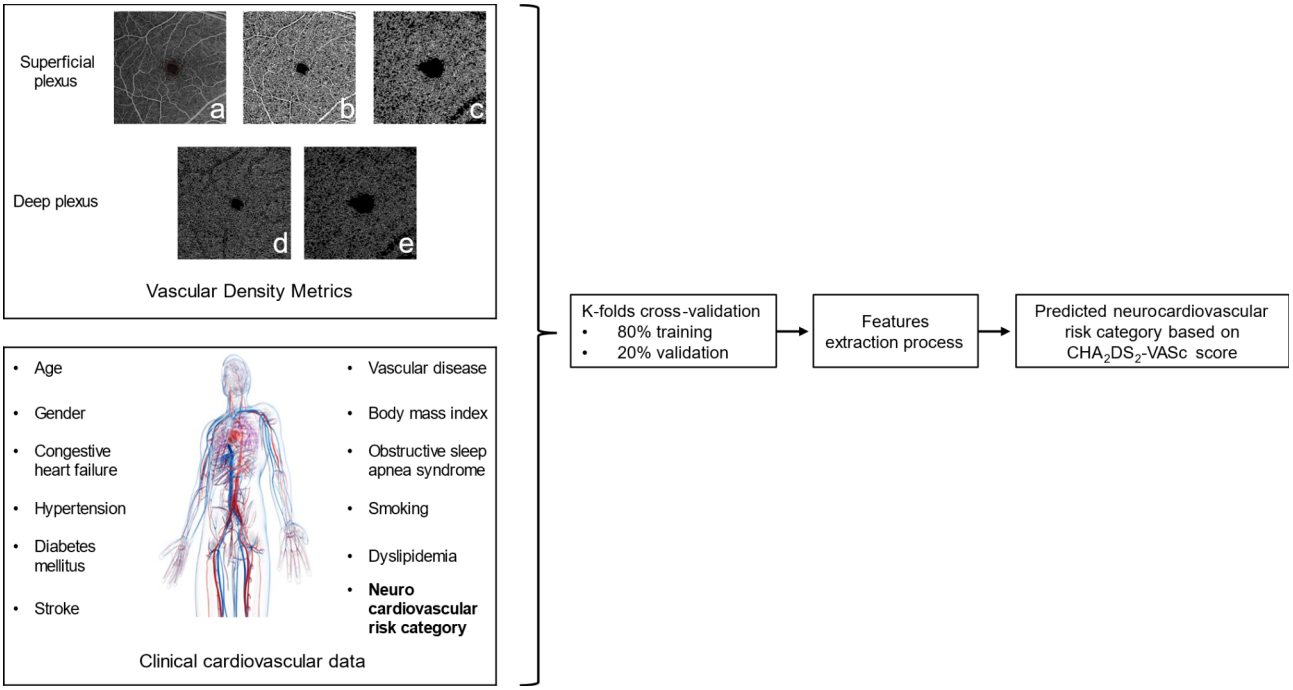

Fig. 2. Schematic illustration of machine-learning model design. (**a**) Angio-retina layer image shows the fovea avascular zone (FAZ) outline with 3 associated measures: area of the FAZ in mm^2, perimeter of the FAZ in mm, and circularity index of the FAZ (ranging from 0 to 1). (**b**) and (**d**) show vessel density, which is defined as the total length of perfused vasculature per unit area in a region of measurement in mm^{-1}. (**c**) and (**e**) show perfusion density, which is defined as the total area of perfused vasculature per unit area in a region of measurement (ranging from 0 to 1). Neurocardiovascular risk category is the target of machine-learning models, it should not be considered as a feature.

Vascular characteristics	Features	
	Superficial plexus	Deep plexus
Fovea avascular zone	Raw length (mm)	
	Circularity (index)	
	Raw size (mm^2)	
Vessel density (mm^{-1})	Density average	Density average
	Density in a circle of 3-mm diameter	Density in a circle of 3-mm diameter
	Density in a circle of 6-mm diameter	Density in a circle of 6-mm diameter
Perfusion density (index)	Perfusion average	Perfusion average
	Perfusion in a circle of 3-mm diameter	Perfusion in a circle of 3-mm diameter
	Perfusion in a circle of 6-mm diameter	Perfusion in a circle of 6-mm diameter

Table 4. Retinal SS OCT-A quantitative parameters used in ML models.

for training a less biased model, where the ratio between the two target classes was the same in each fold as it was in the full dataset. Details on the network implementation are given in Table 5.

Deep-learning network implementation

The entire network was implemented in TensorFlow 2.8 using the EfficientNetV2-B3 backbone from the Keras library. The reported metrics for each model represent the average performance across folds and are detailed in the "Results" section. Training involved 50 epochs with a batch size of 4, a learning rate set to $1e^{-4}$, and the application of weighted sparse categorical cross entropy (CCE) loss. Following the initial training phase, the last 20 layers were unfrozen, and the network underwent an additional 50 epochs of fine-tuning. Since en face SS OCT-A images are grayscale, they were converted to RGB format by triplicating the channel, adhering to EfficientNet's requirement for three-channel images.

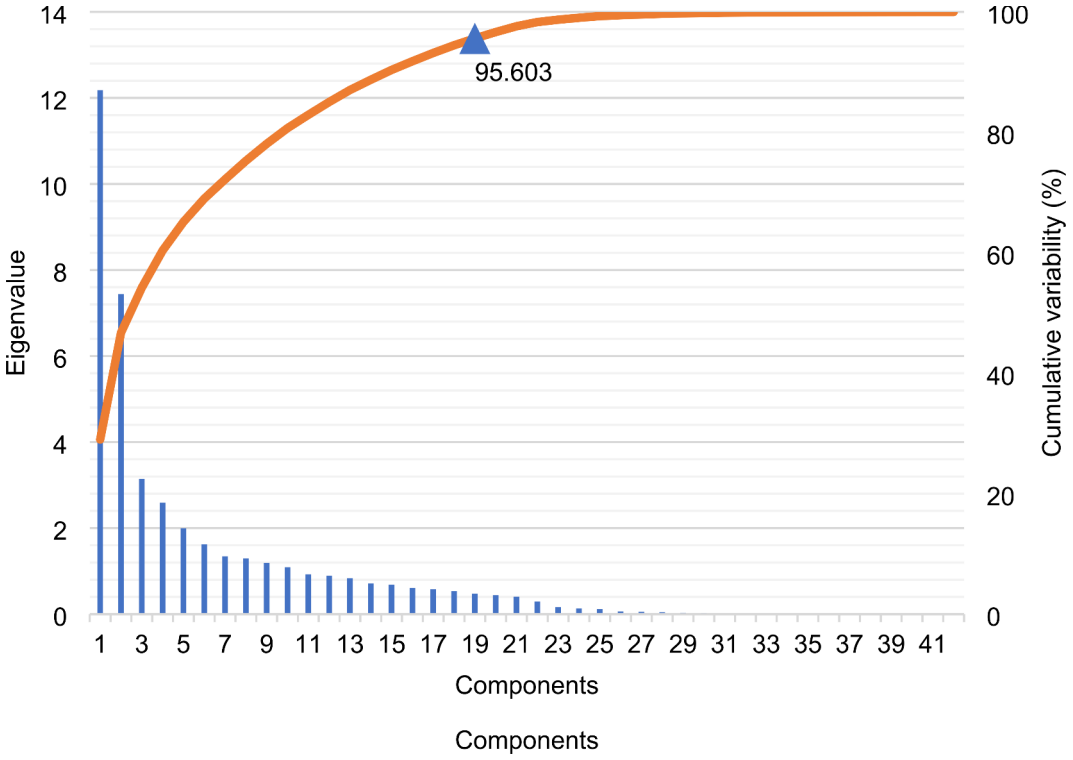

Fig. 3. Scree plot.

Deep-learning model assessment

For the evaluation, we used balanced accuracy as a metric for our imbalanced dataset, which is calculated as the arithmetic mean of sensitivity (true positive rate) and specificity (true negative rate). To assess the performance of the trained EfficientNetV2-B3 network, we performed a comparative analysis employing a random forest (RF) classifier based on the features extracted from the network. Predictions for each image were generated using a truncated version of the trained network, specifically capturing the features inferred at the last dense layer with a kernel size of 32. These features were used to train an RF classifier.

Results

Dataset

Overall, 491 patients were registered in this study. Of the 491 patients, 225 (45.8%) patients had a low neurocardiovascular risk and 266 (54.2%) had an intermediate–high neurocardiovascular risk. The mean age of the patients was 52.4 ± 18.4 years and 51.5% were women. All the cardiovascular clinical data and quantitative SS OCT-A variables were significantly different between the two neurocardiovascular risk categories. A comparison of the clinical and demographic variables is available in the supplementary material (Supplementary Table S1).

Machine-learning model results

The SVM model performed better than the others in predicting neurocardiovascular risk categories (AUC 0.98 ± 0.03 versus 0.96 ± 0.02 and 0.91 ± 0.04 and 0.78 ± 0.12 for logistic regression, RF, and decision tree, respectively). The results are shown in Table 6.

Deep-learning model results

For classifying the two categories, the network was able to achieve a balanced accuracy of 68% as compared to 61% and 54% for Random forest (RF) and Random forest-Features only (RF-FO), respectively. In evaluating the performance of the networks on the test set, the EfficientNet model and both variants of the RF model (RF and RF-FO) exhibited similar results. All the models demonstrated the same mean absolute error (MAE) of approximately 0.697. The R^2 scores for the two models were identical at -0.9446. In terms of balanced accuracy, the EfficientNet model outperformed the RF models, achieving a balanced accuracy of 39%, compared to 33% for both RF variants. Main results are shown in Table 7. The learning curves are presented in the supplementary material (Supplementary Fig. S1). Classification results details are shown in the supplementary material (Supplementary Fig. S2).

Discussion

In this study, we found good results for neurocardiovascular risk category prediction based on retinal SS OCT-A, with a strong predictive accuracy of up to 98% for ML models and 68% for the EfficientNetV2-B3

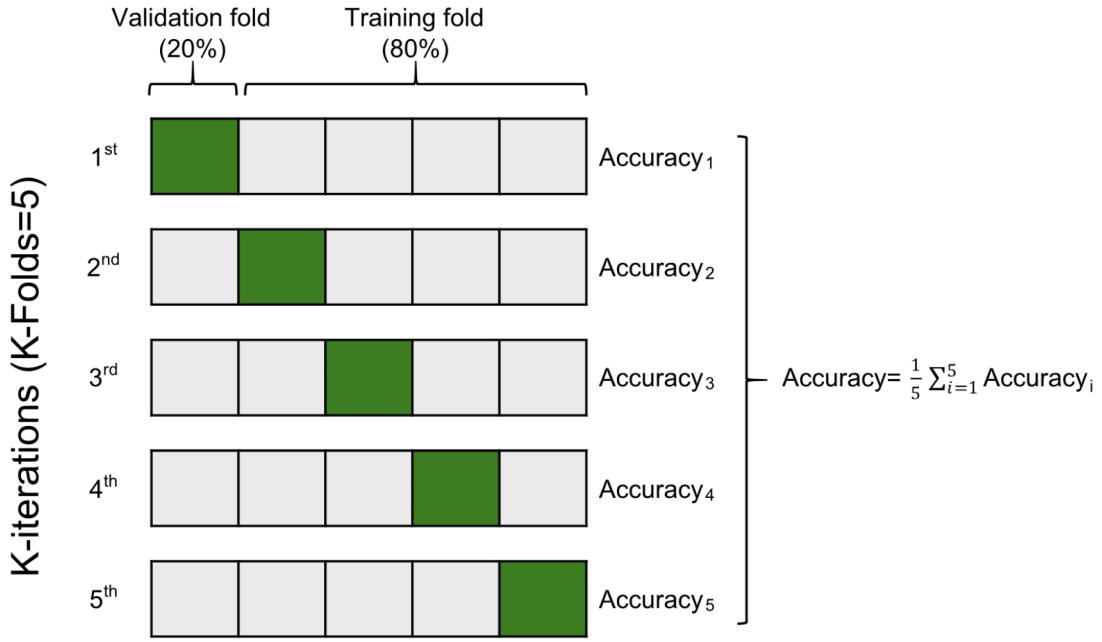

Fig. 4. K-fold cross-validation.

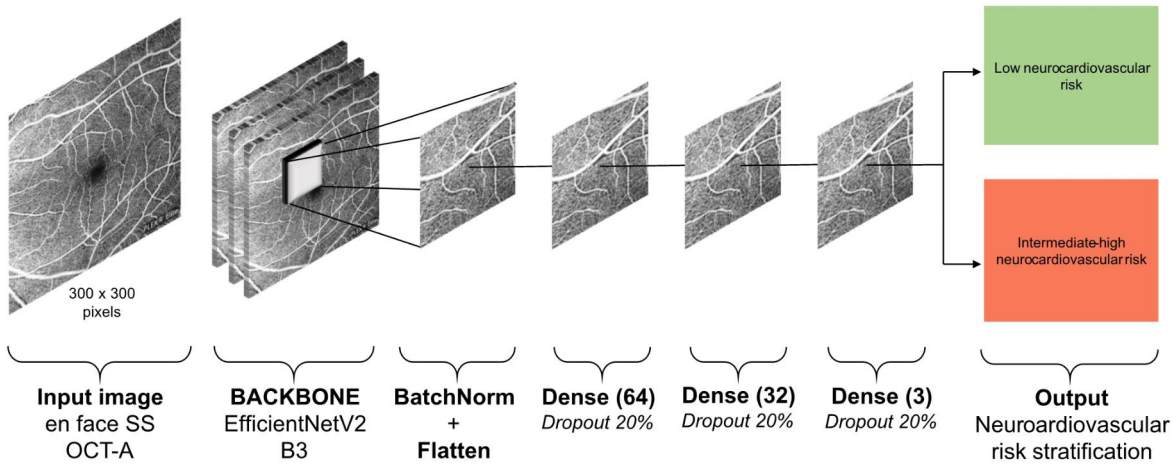

Fig. 5. Deep-learning network based on EfficientNetv2-B3 backbone.

Model used	EfficientNetB3-V2
Image resolution	300
Batch size	16
Epochs	100
K-folds	5
Learning rate	1.00E−03
Fine-tune epochs	50
Fine-tune learning rate	1.00E−03
Loss function	Weighted categorical cross entropy
Early stopping	True
Early stopping patience	25
Labeling methods	One-Hot
Input scaling	0–255
Optimizer	Adamv2
Activation function	ReLU
Cross-validation	Stratified k-folds
Train test splits	20
Pretrained weights	ImageNet
Dense layers	4
Pooling	Average
Dropout	20
Kernel regularizers	L1_L2
Batch norm	Yes
LR scheduler	Yes
Input augmentation	Flip, brightness (25%), saturation (25%)
Ensemble voting	Soft

Table 5. Deep-learning network implementation details.

	Decision tree		Random forest		SVM		Logistic regression	
	AUC	Accuracy (%)	AUC	Accuracy (%)	AUC	Accuracy (%)	AUC	Accuracy (%)
k folds (k = 10)	0.78 ± 0.12	77.2 ± 3.4	0.91 ± 0.04	81.2 ± 2.9	0.98 ± 0.03	85.1 ± 5.9	0.96 ± 0.02	84.9 ± 5.6
k folds (k = 5)	0.77 ± 0.06	75.8 ± 3.0	0.90 ± 0.06	80.8 ± 2.3	0.98 ± 0.02	84.2 ± 5.1	0.96 ± 0.02	84.4 ± 5.2

Table 6. Machine-learning model results. *SVM* support vector machines, *AUC* area under the curve. Descriptive results for models are presented as mean ± standard deviation.

	EfficientNetB3-V2	Random forest	Random forest features only
Balanced accuracy	0.68	0.61	0.54
Accuracy	0.67	0.58	0.52
R^2 score	− 0.3444	− 0.7111	− 0.9556

Table 7. Performance of deep-learning-based model.

backbone model. To our knowledge, this is the first study to investigate artificial intelligence-based prediction of neurocardiovascular risk score with SS OCT-A. Our results highlight the potential value of SS OCT-A as a biomarker of global neurocardiovascular status.

DL methods offer significant advantages over traditional ML methods in predicting neurocardiovascular risk scores from retinal SS OCT-A images. DL models, such as EfficientNetV2-B3, can directly process raw images and automatically extract complex and relevant features, while ML models rely on pre-extracted clinical data and quantitative OCT-A data.

ML models, using both clinical and quantitative data, achieved notable performances as SVM reached an AUC of 0.98 with an accuracy of 85.1%. These results are artificially inflated by the integration of clinical data. The inclusion of clinical data, such as age, gender, diabetes status, and other cardiovascular risk factors, gives these ML models an unfair advantage. These clinical features are directly related to the CHA_2DS_2-VASc score, which means the results are inflated by using data that is inherently predictive of the outcome.

In contrast, DL models in this study were trained using only SS OCT-A images without additional clinical data. This makes the prediction task more challenging but also more indicative of the model's true ability to generalize and find meaningful patterns in the retinal images. The DL model's performance was significantly influenced by the optimization of several hyperparameters, which are crucial for controlling the learning process and ensuring effective training of the model. We chose a learning rate of $1e^{-3}$ (Table 5), which is the step size at each iteration while moving toward a minimum of the loss function, because lower learning rates took a too long training time. The batch size of 16 (Table 5) is the number of training examples utilized in one iteration. A larger batch size would lead to faster training and more stable gradient estimates, but it required too much memory. The number of epochs of 100 determines how many times the learning algorithm will work through the entire training dataset. More epochs didn't improve the model's performance and led to overfitting.

Fine-tuning, which involved adjusting the weights of the last layers of a pre-trained model, significantly improved performance by adapting the model to the specific characteristics of SS OCT-A data. The fine-tune learning rate of $1e^{-3}$ was optimized to maximize learning while avoiding overfitting. Additionally, data augmentation techniques, including flipping and adjusting brightness and saturation, enhanced the model's robustness by helping it generalize to variations in image appearance. Further tests on more powerful computing machines with numerous training and different parameters could lead to better results.

In summary, while ML models show high performance metrics due to the bias introduced by using clinical data, DL methods provide a more unbiased and accurate assessment by relying solely on the image data. This makes DL methods more effective in analyzing complex image data and providing accurate predictions of neurocardiovascular risk scores.

Fundus photography (FP) was the first imaging modality in ophthalmology to prove its value in automatic CV risk assessment. Most hospital departments and practitioners have FP equipment, which has led to the creation of many rich databases such as the UK Biobank and MESSIDOR[31]. These databases, containing hundreds or thousands of fundus images, have been used in several studies to assess and predict CVD. Our results on artificial intelligence-based prediction of neurocardiovascular risk score with SS OCT-A were in line with previous studies based on FP. Poplin et al. used FPs to demonstrate the contribution of retinal vasculature to the automatic detection of CVD and CVD risk factors, where AUC values of DL models were greater than 0.70 and demonstrated their effectiveness in predicting some CVD risk factor and the occurrence of major adverse cardiovascular events (MACE) over a 5-year period[19]. Cheung et al. published their work on the assessment of CVD risk via automatic measurement of retinal-vessel caliber (RVC)[32]. They developed and tested a DL model to specifically measure RVC from more than 70,000 FPs. They assessed the agreement of the RVC measurement between the DL model and a human expert. The DL models predicted CVD risk factors significantly better than the human-based models or were at least comparable[32]. More recently, Zhang et al. demonstrated the capability of DL models to identify chronic kidney disease and diabetes mellitus using 115,344 FPs alone or in combination with clinical metadata (i.e., age, sex, BMI, and blood pressure), with AUCs ranging from 0.85 to 0.93. Additionally, the models could predict glomerular filtration rates and blood glucose levels, yielding MAEs of 11.1–13.4 mL/min per 1.73 m^2 and 0.65–1.1 mmol/L, respectively[33].

However, the exploration of microvasculature at the micrometer level in various plexuses and vascular networks made possible by SS OCT-A could offer hope for an even more accurate and earlier assessment of CV risk compared to FP. Based on previous ophthalmological research, Hassan et al. conducted an evaluation using three-dimensional CNNs to predict the individual age and sex directly from 3D retinal OCT scans, using a large dataset comprising 66,767 participants from the UK Biobank dataset. Model results showed accurate predictions for age (MAE = 3.30 years, R^2 = 0.89) and for sex (AUC = 0.86)[34]. In the same vein, Munk et al. focused on evaluating the performance of DL models in predicting patient age or sex using FPs and OCT scans. Their dataset comprised 135,667 FPs and 85,536 volumetric OCT scans. For sex prediction, the DL models achieved AUC values of 0.80 for FPs, 0.84 for OCT cross sections, and 0.90 for OCT volumes. In terms of age prediction, the input OCT volume models were better than OCT cross sections and better than FPs (MAE = 4.541 years, 5.625 years, and 6.328 years, respectively)[35]. These findings showed the varying predictive capabilities between FPs and OCT scans, where OCT seems to yield a better prediction of CV risk factors. Considering the favorable measurability and the wealth of retinal information offered by OCT, it is expected that OCT-A studies could expand the research on the potential of CV risk assessment. Initial work was undertaken to estimate the CV risk score (American Hospital Association [AHA] risk score, Syntax risk, and SCORE risk score) with ML models based on retinal vascular quantitative parameters measured with FPs and OCT-A scans through a multimodal approach[36]. Using OCT-A data, the K-nearest neighbor (KNN) and the naïve Bayes (NB) approaches more accurately predicted the three CV risk scores, with prediction rates ranging from 76.09 ± 3.08 to 96.13 ± 1.08 for KNN and 76.19 ± 5.30 to 96.23 ± 1.88 for NB. With FP-based vascular parameters, these two ML models also performed better than the others in CV risk assessment, with prediction rates ranging from 70.54 ± 8.56 to 95.83 ± 1.19 for KNN and 74.36 ± 6.17 to 96.28 ± 1.21 for NB. When combining both FP and OCT-A quantitative data, NB was the best fitted model, with an accuracy ranging from 75.64 ± 5.96 to 96.53 ± 1.25[36]. Concurrently, Zhong et al. investigated the prediction of coronary artery disease using a combination of clinical, electrocardiographic (ECG), and OCT-A data. The model trained on the combined clinical, ECG, and OCT-A data was presented as the individual prediction nomogram, exhibiting good discrimination (AUC = 0.897 [95% CI 0.861–0.933]). Notably, the OCT-A model outperformed the ECG model in predicting individuals with coronary heart disease (AUC = 0.730 [95% CI 0.673–0.788])[37].

Research in CV risk assessment using SS OCT-A was held back by the lack of data. In fact, only a few datasets such as the OCTAGON and FOCTAIR datasets[38], the Retinal OCTA SEgmentation dataset (ROSE)[39], and OCTA-500[40] were publicly available. However, none of these datasets combined the OCT-A scans with the CV data of the patients included. We therefore chose to use the RASTA dataset, the first open-source dataset that combined clinical CV data and SS OCT-A scans. To the best of our knowledge, using this database enabled us

to be the first research team to focus on predicting the neurocardiovascular risk category from SS OCT-A. This retinal imaging modality provides precise quantitative measurements of vascular density and blood perfusion, unlike FPs where assessment of vascular flow is not possible. Moreover, SS OCT-A has made it possible to explore the chorioretinal vasculature in much greater depth than PFs, enabling visualization of the anatomical vascular layers, i.e., the superficial and deep plexuses. The other major advantage is that this approach could monitor the evolution of lesions by allowing for repeated examinations, thereby assessing the effectiveness of treatments and the progression of the CVD. Although there were several ways to quantify the density of the retinal vasculature, the 15 quantitative datasets used to train our models could be considered a comprehensive representation of retinal microvasculature complexity because they included an analysis of the foveal avascular zone (FAZ), perfusion, and vascular density in a central area of 3×3 and 6×6 mm. In our study we found that the ML models performed better than the CNN model; however, our CNN model only had SS OCT-A scans as input, unlike the ML models that combined raw data of 11 CV risk factors. Therefore, we could have obtained better DL results in our study if we had included other CV risk factors in the algorithm.

The models exhibited a consistent absolute prediction error (MAE = 0.697) and strong negative correlation ($R^2 = -0.9446$).

A major limitation of our study was the small sample size compared to FP-based algorithms and consisted solely of European individuals. In addition, there is an unbalanced sex ratio in the low and intermediate-high neurocardiovascular risk groups, with more women in the low-risk group and more men in the intermediate-high risk group. However, this distribution could be representative and appears to reflect real-life conditions regarding each person's CHA_2DS_2-VASc score. The generalizability of our models beyond the RASTA dataset requires further validation on larger external datasets with different ethnic groups. Second, our dataset was based on a specific SS OCT-A device (PLEX Elite 9000®, Carl Zeiss Meditec Inc., Dublin, OH, USA), which could limit our results with other manufacturers. This is indeed a limiting factor of our algorithm, which should be tested on retinal images from other OCT-A devices to improve the generalizability of our model. This should be tested in another work with this algorithm. Furthermore, longitudinal follow-up of neurocardiovascular events could strengthen our results.

The ML and DL models described in this study accurately predicted the CHA_2DS_2-VASc score. The models were validated on a public dataset that registers patients with different CV risk factors. The models achieved good performance and, thanks to their SS OCT-A evaluation, may improve the management of patients referred to ophthalmologists. For the generalizability of our results, it is a priority to validate the models in future studies.

Data availability

The RASTA dataset is hosted and publicly available at https://rasta.u-bourgogne.fr/.

Received: 25 April 2024; Accepted: 1 November 2024
Published online: 07 November 2024

References

1. WHO. *World Health Organization Reveals Leading Causes of Death and Disability Worldwide: 2000–2019*. https://www.who.int/news/item/09-12-2020-who-reveals-leading-causes-of-death-and-disability-worldwide-2000-2019 (2020).
2. Goff, D. C. Jr. et al. 2013 ACC/AHA guideline on the assessment of cardiovascular risk: a report of the American College of Cardiology/American Heart Association Task Force on Practice Guidelines. *Circulation* **129**, S49–S73. https://doi.org/10.1161/01.cir.0000437741.48606.98 (2014).
3. Anderson, K. M., Wilson, P. W., Odell, P. M. & Kannel, W. B. An updated coronary risk profile. A statement for health professionals. *Circulation*. **83**, 356–362. https://doi.org/10.1161/01.cir.83.1.356 (1991).
4. group, S. W. & , E. C. R. SCORE2 risk prediction algorithms: new models to estimate 10-year risk of cardiovascular disease in Europe. *Eur. Heart J.* **42**, 2439–2454. https://doi.org/10.1093/eurheartj/ehab309 (2021).
5. Lin, B. et al. Cumulative risk of stroke recurrence over the last 10 years: a systematic review and meta-analysis. *Neurol. Sci.* **42**, 61–71. https://doi.org/10.1007/s10072-020-04797-5 (2021).
6. Jokhadar, M., Jacobsen, S. J., Reeder, G. S., Weston, S. A. & Roger, V. L. Sudden death and recurrent ischemic events after myocardial infarction in the community. *Am. J. Epidemiol.* **159**, 1040–1046. https://doi.org/10.1093/aje/kwh147 (2004).
7. Arnould, L. et al. The EYE-MI pilot study: a prospective acute coronary syndrome cohort evaluated with retinal optical coherence tomography angiography. *Investig. Ophthalmol. Vis. Sci.* **59**, 4299–4306. https://doi.org/10.1167/iovs.18-24090 (2018).
8. Spaide, R. F., Klancnik, J. M. Jr. & Cooney, M. J. Retinal vascular layers imaged by fluorescein angiography and optical coherence tomography angiography. *JAMA Ophthalmol.* **133**, 45–50. https://doi.org/10.1001/jamaophthalmol.2014.3616 (2015).
9. Mariampillai, A. et al. Speckle variance detection of microvasculature using swept-source optical coherence tomography. *Opt. Lett.* **33**, 1530–1532. https://doi.org/10.1364/ol.33.001530 (2008).
10. Huang, Y. et al. Swept-source OCT angiography of the retinal vasculature using intensity differentiation-based optical microangiography algorithms. *Opthalmic Surg. Lasers Imaging Retin.* **45**, 382–389. https://doi.org/10.3928/23258160-20140909-08 (2014).
11. Stanga, P. E. et al. Swept-source Optical Coherence Tomography Angio™ (Topcon Corp, Japan): Technology review. *Dev. Ophthalmol.* **56**, 13–17. https://doi.org/10.1159/000442771 (2016).
12. Jia, Y. et al. Split-spectrum amplitude-decorrelation angiography with optical coherence tomography. *Opt. Express.* **20**, 4710–4725. https://doi.org/10.1364/oe.20.004710 (2012).
13. Laíns, I. et al. Retinal applications of swept source optical coherence tomography (OCT) and optical coherence tomography angiography (OCTA). *Prog. Retin Eye Res.* **84**, 100951. https://doi.org/10.1016/j.preteyeres.2021.100951 (2021).
14. Lip, G. Y., Nieuwlaat, R., Pisters, R., Lane, D. A. & Crijns, H. J. Refining clinical risk stratification for predicting stroke and thromboembolism in atrial fibrillation using a novel risk factor-based approach: the euro heart survey on atrial fibrillation. *Chest.* **137**, 263–272. https://doi.org/10.1378/chest.09-1584 (2010).
15. Wagner, S. K. et al. Insights into systemic disease through retinal imaging-based Oculomics. *Transl. Vis. Sci. Technol.* **9**, 6. https://doi.org/10.1167/tvst.9.2.6 (2020).
16. Arnould, L. et al. Using artificial intelligence to analyse the retinal vascular network: the future of cardiovascular risk assessment based on oculomics? A narrative review. *Ophthalmol. Ther.* **12**, 657–674. https://doi.org/10.1007/s40123-022-00641-5 (2023).

17. Khan, S. M. et al. A global review of publicly available datasets for ophthalmological imaging: barriers to access, usability, and generalisability. *Lancet Digit. Health*. **3**, e51–e66. https://doi.org/10.1016/s2589-7500(20)30240-5 (2021).
18. Germanèse, C. et al. A retinal Oct-Angiography and Cardiovascular STAtus (RASTA) dataset of swept-source microvascular imaging for cardiovascular risk assessment. *Data*. **8**, 147 (2023).
19. Poplin, R. et al. Prediction of cardiovascular risk factors from retinal fundus photographs via deep learning. *Nat. Biomed. Eng.* **2**, 158–164. https://doi.org/10.1038/s41551-018-0195-0 (2018).
20. Rudnicka, A. R. et al. Artificial intelligence-enabled retinal vasculometry for prediction of circulatory mortality, myocardial infarction and stroke. *Br. J. Ophthalmol.* **106**, 1722–1729. https://doi.org/10.1136/bjo-2022-321842 (2022).
21. Sun, Z., Yang, D., Tang, Z., Ng, D. S. & Cheung, C. Y. Optical coherence tomography angiography in diabetic retinopathy: an updated review. *Eye (London England)*. **35**, 149–161. https://doi.org/10.1038/s41433-020-01233-y (2021).
22. Monteiro-Henriques, I., Rocha-Sousa, A. & Barbosa-Breda, J. Optical coherence tomography angiography changes in cardiovascular systemic diseases and risk factors: a review. *Acta Ophthalmol.* **100**, e1–e15. https://doi.org/10.1111/aos.14851 (2022).
23. Aker, A., Volis, I., Saliba, W., Naoum, I. & Zafrir, B. CHA2DS2-VASc score as a predictor of adverse outcomes after ischemic stroke in patients without Atrial Fibrillation. *Isr. Med. Assoc. J. IMAJ*. **26**, 143–148 (2024).
24. Melgaard, L. et al. Assessment of the CHA2DS2-VASc score in predicting ischemic stroke, thromboembolism, and death in patients with heart failure with and without atrial fibrillation. *JAMA*. **314**, 1030–1038. https://doi.org/10.1001/jama.2015.10725 (2015).
25. Su, C. H. et al. CHA2DS2-VASc score as an independent outcome predictor in patients hospitalized with acute ischemic stroke. *PLoS One*. **17**, e0270823. https://doi.org/10.1371/journal.pone.0270823 (2022).
26. Guerra, F. et al. CHA(2)DS(2)-VASc risk factors as predictors of stroke after acute coronary syndrome: a systematic review and meta-analysis. *Eur. Heart J. Acute Cardiovasc. Care*. **7**, 264–274. https://doi.org/10.1177/2048872616673536 (2018).
27. Tu, H. T. et al. Pre-stroke CHADS2 and CHA2DS2-VASc scores are useful in stratifying three-month outcomes in patients with and without atrial fibrillation. *Cerebrovasc. Dis.* **36**, 273–280. https://doi.org/10.1159/000353670 (2013).
28. Xing, Y. et al. CHA(2)DS(2)-VASc score as a predictor of long-term cardiac outcomes in elderly patients with or without atrial fibrillation. *Clin. Interv. Aging*. **13**, 497–504. https://doi.org/10.2147/cia.s147916 (2018).
29. Akboğa, M. K., Yılmaz, S. & Yalçın, R. Prognostic value of CHA2DS2-VASc score in predicting high SYNTAX score and in-hospital mortality for non-ST elevation myocardial infarction in patients without atrial fibrillation. *Anatol. J. Cardiol.* **25**, 789–795. https://doi.org/10.5152/AnatolJCardiol.2021.03982 (2021).
30. Tan, M. & Le, Q. EfficientNet: Rethinking Model Scaling for Convolutional Neural Networks. *Int. Conference Machine Learning*. 6105–6114 (2019).
31. Decencière, E. et al. Feedback on a publicly distributed image database: The messidor database. *Image Anal. Stereol.* https://doi.org/10.5566/ias.1155 (2014).
32. Cheung, C. Y. et al. A deep-learning system for the assessment of cardiovascular disease risk via the measurement of retinal-vessel calibre. *Nat. Biomed. Eng.* **5**, 498–508. https://doi.org/10.1038/s41551-020-00626-4 (2021).
33. Zhang, K. et al. Deep-learning models for the detection and incidence prediction of chronic kidney disease and type 2 diabetes from retinal fundus images. *Nat. Biomed. Eng.* **5**, 533–545. https://doi.org/10.1038/s41551-021-00745-6 (2021).
34. Hassan, O. et al. Deep learning prediction of age and sex from optical coherence tomography. In *IEEE 18th International Symposium on Biomedical Imaging (ISBI)*., 238–242 (IEEE, 2021).
35. Munk, M. R. et al. Assessment of patient specific information in the wild on fundus photography and optical coherence tomography. *Sci. Rep.* **11**, 8621. https://doi.org/10.1038/s41598-021-86577-5 (2021).
36. Arnould, L. et al. Prediction of cardiovascular parameters with supervised machine learning from Singapore I vessel assessment and OCT-angiography: a pilot study. *Transl. Vis. Sci. Technol.* **10**, 20. https://doi.org/10.1167/tvst.10.13.20 (2021).
37. Zhong, P. et al. Development and validation of retinal vasculature nomogram in suspected angina due to coronary artery disease. *J. Atheroscler. Thromb.* **29**, 579–596. https://doi.org/10.5551/jat.62059 (2022).
38. *VARPA Working fields: Public databases*. http://www.varpa.es/research/ophtalmology.html#octagon.
39. Ma, Y. et al. A retinal OCT-angiography vessel segmentation dataset and new model. *IEEE Trans. Med. Imaging*. **40**, 928–939. https://doi.org/10.1109/tmi.2020.3042802 (2021).
40. Li, M. et al. OCTA-500: a retinal dataset for optical coherence tomography angiography study. *Med. Image. Anal.* **93**, 103092. https://doi.org/10.1016/j.media.2024.103092 (2024).

Acknowledgements

We would like to thank Professor Ramin Tadayoni and Professor Aude Couturier for sharing data regarding the EVIRED study in Dijon.

Author contributions

All authors contributed to the study conception and design. Material preparation, data collection, and analysis were performed by G.C. Model development was performed by G.C. and A.A. The first draft of the manuscript was written by G.C. and all authors commented on previous versions of the manuscript. All authors read and approved the final manuscript.

Declarations

Competing interests

The authors declare no competing interests.

Additional information

Supplementary Information The online version contains supplementary material available at https://doi.org/10.1038/s41598-024-78587-w.

Correspondence and requests for materials should be addressed to L.A.